Boundary-Layer Flow on a Rotary Vane

H. E. McCARTHY and J. H. OLSON

Department of Chemical Engineering
University of Delaware, Newark, Delaware 19711

The boundary-layer flow on a rotating vane is investigated with the integral momentum approximation. A parabolic velocity profile is approached over a significant portion of the vane. The assumption of a parabolic velocity profile yields a closed analytical solution for the radial dependence of the surface velocity. Experimental data obtained agree with the predicted average velocity at the exit of the vane.

In the chemical industry there are many applications for centrifugal dispersers such as those used in spray drying and pelletizing. The present study was undertaken to achieve a better understanding of the flow conditions on a vane of a disc atomizer. In some applications both the shear history of the fluid and the exit velocity can be important. For example, Turner and McCarthy (5) have shown that the degree of dispersion of solids or immiscible liquids is a function of the shear stress produced in the fluid.

This study uses an integral momentum attack upon the flow on a partially filled rotating vane. Other workers have considered similar problems. Hallern et al. (3) examined the boundary-layer flow on curved vanes. Their work differs from the present study because they considered the boundary-layer flow for submerged vanes. In addition Marshall (4) considered the boundary-layer flow in a thin film on a rotating vane. A parabolic velocity profile was assumed for a fluid in laminar flow. For turbulent flow Marshall used a friction factor with the assumption of constant fluid height on the vane. For the laminar flow case, Marshall's equation for the average velocity on the vane is

$$V'_r \frac{dV'_r}{dr} + 3\nu' \frac{h'^2_v}{Q'^3} V'^3_r - \omega'^2 r' = 0$$

This solution assumes that the form of the velocity profile is independent of radial position; the validity of this assumption is investigated in this effort. Both attacks lead to numerical integration of an ordinary differential equation as the basis for solution.

THEORY

In this section the equations for the boundary-layer flow on a vane are developed. Then the equation for the position of the fluid after it leaves the vane is considered. The latter result is needed to compare experimental data with predicted values. The data will be discussed in a later section.

Boundary-Layer Flow on a Vane

Figure 1 shows a scheme of the vane, the fluid flow, and pertinent nomenclature. The fluid is incompressible and Newtonian.

In dimensionless form the equation of motion in a coordinate system rotating with the vane is

$$V_r \frac{\partial V_r}{\partial r} + V_h \frac{\partial V_r}{\partial h} = r + \frac{1}{N} \frac{\partial^2 V_r}{\partial h^2} \qquad (1)$$

where V_h is the angular velocity relative to the rotating vane and h is a small distance normal to the vane.
The continuity equation yields for V_h

$$V_h = -\int_0^h \left(\frac{V_r}{r} + \frac{\partial V_r}{\partial r} \right) dh' \qquad (2)$$

The h coordinate can be replaced with a η coordinate which goes from zero at the surface of the vane to unity at the free surface of the liquid on the vane. Thus the dimensionless depth of the fluid on the vane $h_V(r)$ is needed as a parameter of the problem. The radial fluid velocity V_r *is* written in terms of the surface velocity and a profile function:

$$V_r(r, h) = S(r)\phi(r, h/h_v) = S(r)\phi(r, \eta) \qquad (3)$$

where $S(r)$ is free surface fluid velocity, $\phi(r, \eta)$ is the velocity profile function, and $\eta = h/h_r$ is the liquid depth coordinate. The continuity of flow upon the vane yields a simple relation for h_v in terms of the total flow per unit vane width Q

$$Q = \int_0^{h_v} V_r \, dh' = h_v \int_0^1 V_r \, d\eta \qquad (4a)$$

Thus

$$h_v = Q/SA \qquad (4b)$$

where $A = \int_0^1 \phi(r, \eta) \, d\eta$ is the ratio of the average velocity in the vane to the surface velocity.

Introduction of Equations (2) to (4*b*) into Equation (1) yields the fundamental statement of the problem:

$$V_r \frac{\partial V_r}{\partial r} - \frac{\partial V_r}{\partial \eta} \int_0^\eta \left(\frac{V_r}{r} + \frac{\partial V_r}{\partial r} \right) d\eta' = r + \frac{S^2 A^2}{Q^2 N} \frac{\partial^2 V_r}{\partial \eta^2} \qquad (5)$$

The new feature of this work is to recognize that h_v and

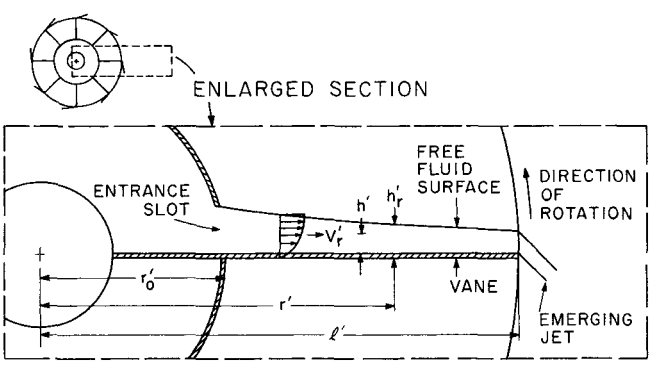

Fig. 1. Free flow on a rotating vane.

H. E. McCarthy is at Garret Research, LaVerne, California 91750. Correspondence concerning this paper should be addressed to J. H. Olson.

consequently ϕ are functions of radial position. The dependence upon raidal position becomes clear when $\phi(r, \eta)$ is approximated by a simple polynomial. The third-order von Karman-Pohlhausen approximation for the velocity profile is determined from four boundary conditions:

$\phi(r, 0) = 0$	no slip at the surface of the vane
$\phi(r, 1) = 1$	surface velocity at $\eta = 1$
$\frac{\partial \phi}{\partial \eta}(r, 1) = 0$	no shear at liquid-gas interface
$\frac{\partial \phi^2}{\partial \eta^2}(r, 0) = -\frac{rQ^2N}{S^3A^2}$	Equation (5) at the vane surface

Consequently the ϕ function becomes

$$\phi(r, \eta) = \left(\frac{3}{2}\eta - \frac{1}{2}\eta^3\right) + G\left(\frac{\eta}{4} - \frac{\eta^2}{2} + \frac{\eta^3}{4}\right) \quad (6)$$

$$G = \frac{rQ^2N}{A^2S^3}$$

Equation (5) is reduced to an ordinary differential equation by integrating (averaging) across the flow on the vane. The equation prior to substitution of the particular velocity profile approximation becomes

$$\int_0^1 \frac{1}{r}\frac{\partial V_r^2 r}{\partial r}\,d\eta - S\int_0^1 \frac{1}{r}\frac{\partial (V_r r)}{\partial r}\,d\eta = r - \frac{r}{G}\frac{\partial V_r}{\partial \eta}\Bigg|_0 \quad (7)$$

The remainder of the development is simple but tedious algebra; the polynomial expression for V_r is introduced into Equation (7) and reduced to a first-order ordinary differential equation for S. The final form of this equation is

$$\frac{dS}{dr}\frac{1}{P_1}\left(rP_2 - \frac{P_3}{r}\right) \quad (8)$$

where

$$P_1 = \frac{GS}{1680}(582 + 41G + 2G^2) - \frac{10}{10+G}(-234 + 3G + G^2) - \frac{30+G}{10+G}(3G + 2G^2)$$

$$P_2 = G - \frac{S}{4}(3 + G)$$

$$P_3 = \frac{GS^2}{1680}(-234 + 3G + 3G^2)$$

G is the positive root of the polynomial.

$$G^3 + 60G^2 + (30)^2 G - (48)^2 r\frac{Q^2N}{S^3} = 0$$

The initial value of S is an unknown in this development. However if the polynomial profile is established at the flow entrance to the vane, the initial velocity is found from the approximation

$$S_0 = \frac{h_0^2 N r_0}{30} - \frac{8}{5}$$

where h_0 is the thickness of the the slot which conveys the fluid to the vane at r_0. Since the von Karman-Pohlhausen velocity profile probably is not established at the vane entrance, S_0 is unknown. The initial value S_0 therefore will be treated as an adjustable parameter and the implications of this approach will be discussed later. It will be shown that use of a parabolic velocity profile will give an adequate estimate for the initial surface velocity.

Fluid Path at the Edge of the Vane

In order to analyze the experimental data it is necessary to find the path of a fluid element after leaving the vane. For this analysis it is assumed that there is no air drag on the free fluid jet exiting from the vane. Experiments discussed later show that good vacuum is required. The velocity of the fluid leaving the vane is assumed to be the average velocity of the fluid. This assumption appears reasonable by comparison to the acceleration of a laminar jet. Duda and Vrentas (*1*) show that for Reynolds numbers above 200 the distance (Z′) to achieve average velocity can be found from $Z'/R'_0 = 5 \times 10^{-2} \times N_{Re}$ (R'_0 is the radius of the exiting jet). If this were valid for our Reynolds numbers, Z′ would be equal to 3×10^{-4} in. The data of Goren and Wronski (*2*) show that $Z'/R'_0 < 1$. For our case this would be $Z' < 1.2 \times 10^{-2}$ in. In both cases the distance is negligibly small.

The apparent jet trajectory and the fluid particle path are indicated on Figure 2. Denoting the origin of the free jet as zero angle, we find the apparent angle θ_f and radial position r. The radial velocity is found by integrating the equation of motion in laboratory coordinates. With the aid of conservation of angular momentum, this velocity is

$$V_r = \left[V_1^2 + 1 - \frac{1}{r^2}\right]^{1/2} \quad (10)$$

where V_1 = the average velocity at the vane exit. The time required to reach the radial position R is found by integrating Equation (10):

$$t = (\omega' t') = \frac{(Br^2 - 1)^{1/2} - V_1}{B}$$

= dimensionless time to reach r (11)

$$B = 1 + V_1^2$$

Equation (11) can be regarded as a parametric equation for the radial position in which negative t is the angular position at which the fluid element exited from the vane. The angular position is found by substituting r^2 from Equation (11) into the differential equation

$$\frac{d\theta}{dt} = \frac{V_\theta}{r} = \frac{1}{r^2} \quad (12)$$

Consequently the parametric form of the apparent jet is

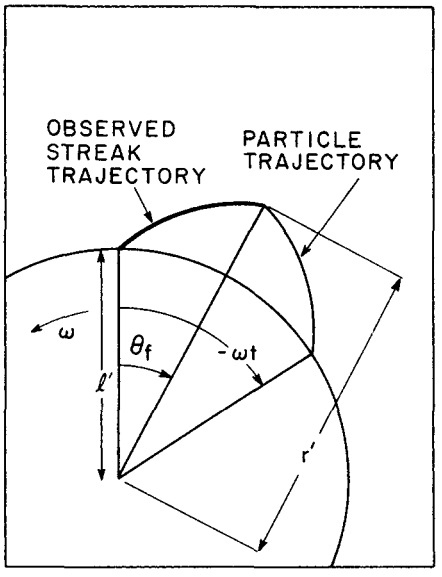

Fig. 2. Trajectory of fluid emerging from vane.

TABLE 1. EXPERIMENTAL DATA

Run	Wheel rev./min.	Pressure, torr	Measured exit velocity, ft./sec.	Calculated exit velocity, ft./sec.
1	600	540	less than 1	3.45
2	600	360	less than 1	3.45
3	600	130	3.5 to 4.0	3.45
4	600	25	3.5 to 4.0	3.45
5	600	10	3.5 to 4.0	3.45
6	600	10	3.5	3.45
7	900	510	less than 1	4.53
8	900	10	4.0 to 4.5	4.53
9	1,200	25	5.0 to 5.5	5.49
10	1,200	50	5.5 to 6.0	5.49
11	1,200	25	5.5 to 6.0	5.49
12	1,200	10	5.5 to 6.0	5.49
13	1,200	10	5.5 to 6.0	5.49

Note: Inside radius 3⅝in., outside radius 7 in., vane depth 7/16 in. Flow rate 4.8 cc./sec. vane, for 10 poise, Dow Corning 200 silicone oil. The measured wheel rev./min. differed from these nominal values by inconsequential amounts.

given as

$$r = \left[\frac{(B1t + V_1)^2 + 1}{B} \right]^{1/2} \qquad (13a)$$

$$\theta_f = -t + \tan^{-1}(Bt + V_1) - \tan^{-1}(V_1) \qquad (13b)$$

Thus the apparent jet trajectory can be found as a simple function of the average exit velocity when fluid drag and surface tension effects are unimportant.

EXPERIMENTAL EQUIPMENT AND PROCEDURE

The experiments conducted in this work yield the average radial velocity of the fluid leaving the vane rather than a direct measure of the velocity profile on the vane. In order to determine the average velocity consistent with Equation (8), photographs of the fluid leaving the vane were taken. The measured fluid trajectories were compared to predicted trajectories.

Equipment

The experimental equipment consisted of a 14-in. diam. wheel with 7/16 in. high vanes. The vanes were tapered slightly to about ⅜ in. at the injected radius. The wheel was covered with Lucite, and a Lucite ring was installed at the inside radius to direct the flow to the two active vanes. These vanes were spaced 180 deg. apart. The inside radius of the vanes was 3⅝ in. The fluid was fed to the vanes through a tube in contact with the wheel near the wheel center. The fluid flow was metered using a variable-speed gear pump. The flow rate was reproducible within 2%.

The wheel was mounted in an 18-in. diam. 25-gal. vacuum tank. The tank cover was equipped with a Teflon shaft seal to allow rotation of the wheel at 10 torr or less, and a plate glass window through which pictures could be taken. The wheel was driven at 600, 900, and 1,200 rev./min. by a large radial drill press. Dow Corning (200 fluid) 10-poise silicon oil was selected for the tests because of the low vapor pressure requirements. The mechanical vacuum pump was capable of maintaining a pressure considerably less than 10 torr. A General Radio Strobatac was used for a photographic light source and to measure the rotational speed of the wheel. The photographs were taken using a Polaroid camera with 3,000 ASA speed film.

The fluid flow was limited 9.6 cc./sec. since significantly higher flows could not be handled by the vane and significantly lower flows could not be supplied dependably.

The pictures of the fluid trajectories were blown up to a standard size and compared to a set of overlays of computed trajectories. The comparison was done visually with a light box to give the best fit to a particular velocity.

EXPERIMENTAL DATA

The calculated fluid trajectories drawn on the overlays were evaluated in 0.5 ft./sec. increments for exit velocities in the range of 1.0 to 10.0 ft./sec. The fluid trajectories are not sensitive enough to exit velocity to allow comparison at velocities spaced closer than 0.5 ft./sec. Thus in Table 1 the observed exit velocities sometimes list two values which fit the data equally well. Consequently a realistic estimate of the experimental errors in our measurements is 0.5 ft./sec.

Table 1 lists the data obtained by measurement and the calculated velocity for three rotational speeds. In experiments 1 to 6 the effect of system pressure was investigated. The trajectories apparently were unaffected by air drag for our measurement method when the system pressure is below 130 torr. Useless results are obtained at atmospheric pressure.

The remainder of Table 1 lists the data observed at 900 and 1,200 rev./min. The measured data appear to fit the model within the precision of the measurements. Although the data presented here are not a direct conformation of our model, they are consistent with our analysis. Consequently it is useful to explore computed results for a wider range of experimental conditions.

COMPUTATIONAL RESULTS—PARAMETER INVESTIGATION

The computations discussed in this section, as well as those used to compute the fluid trajectories, were performed on an S.D.S. 9300 digital computer. Equation (8) was integrated numerically using a Runga-Kutta integration scheme with a variable step size error control. A relative error criterion of 10^{-6} was used.

Computational results in this section represent higher

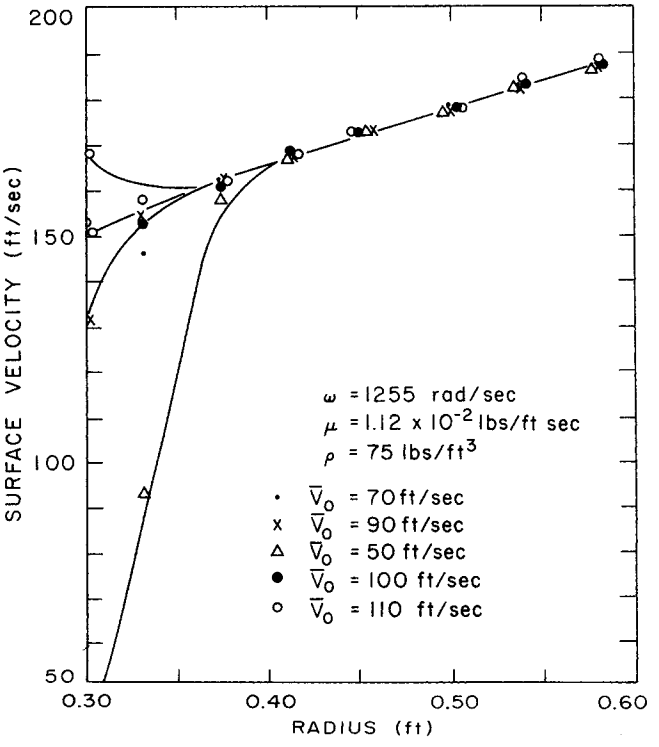

Fig. 3. Effect of inlet velocity on surface velocity.

peripheral velocities than those used for experimental data. These velocities are more akin to those used in commercial practice. This section comprises a discussion of the effect of initial velocity; the behavior of the parameter G, and the influence of operating parameters on surface velocity and shear stress.

The Effect of Initial Velocity

Since initial surface velocity is unknown, it must be treated as an adjustable parameter. Figure 3 shows the surface velocity development for various inlet velocities. It appears from these data that the initial acceleration or deceleration is very strong; consequently the final fluid surface velocity is not dependent on the choice of the initial surface velocity.

Since G is the root of a simple cubic equation, arbitrary specification of S_0 is equivalent to the selection of different values of G. The value of G was within the range $G = 2 \pm 0.02$ for all initial values of S_0 shown on Figure 3 for radial position greater than 0.42 ft. Thus the parameter G approaches 2 quite rapidly.

The Behavior of the Parameter G

The parameter G ($G = Q^2N_r/A^2S^3$) embodies the new feature of this work as a perturbation of the standard quadratic velocity profile. Table 2 shows how the velocity profile is altered by the parameter G. This parameter ranged in the computations from 1 to 3 and approached 2 near the vane exit. When G is 2 the parabolic velocity profile used by Marshall (*4*) is obtained.

Since G approaches 2, it is of interest to explore the implication of a parabolic velocity profile. From the boundary condition, or by setting $G = 2$ in the system equations, one obtains

$$h'_v = \left(\frac{2\nu S}{\omega\rho}\right)^{1/2} = \left(\frac{2\nu' S}{\omega' r}\right)^{1/2} \tag{14}$$

The equation for S is

$$3S\frac{dS}{ar} - \frac{S^2}{r} = 0 \tag{15}$$

which gives

$$S = S_0\left(\frac{r}{r_0}\right)^{1/3} \tag{16a}$$

The initial velocity is obtained from the flow rate and Reynolds number as

$$S_0 = \left(\frac{9Q^2Nr_0}{8}\right)^{1/3} \tag{16b}$$

The solution of Equation (8), with Equation (16*b*) as the boundary condition, deviated from Equation (16*a*) by no more than 2% for a substantial group of tests at realistic conditions. Consequently Equation (16*a*) provides an adequate engineering description of flow upon a rotating vane.

Marshall's monograph (*4*) provides extensive graphical comparison of the average velocity of the fluid on the vane as a function of the design parameters for disc atomizers. The average velocity is two-thirds of the surface velocity when G is 2. Consequently one finds in dimensional form

$$S' \alpha (q')^{2/3}(\omega')^{2/3}(\nu')^{-1/3}(r')^{1/3} \tag{16c}$$

or in terms of the peripheral velocity $(\omega' r')$

$$S' \alpha (\omega' r')^{2/3} r'^{-1/3} \tag{16d}$$

Equations provide a useful compression of information previously described graphically.

Table 2. Parameter G for Range of Values Studied

G	ϕ (boundary-layer polynomial)			
0	$\frac{3}{2}\eta$		$-\frac{1}{2}\eta^3$	(cubic)
1	$\frac{7}{4}\eta$	$-\frac{1}{2}\eta^2$	$-\frac{1}{4}\eta^3$	
2	2η	$-\eta^2$		(parabolic)
3	$\frac{9}{4}\eta$	$-\frac{3}{2}\eta^2$	$-\frac{1}{4}\eta^3$	

The shear stress is important for the processing of shear degradable materials, emulsions, and dispersions. Viscous heating is significant at high shear stress and can be considered by extension of this work. The shear stress is found from the definition

$$\tau' g'_c = \mu' \frac{\partial V'_\tau}{\partial h'} \tag{17}$$

Upon substitution of the dimensionless parameters and simplification

$$(\tau' g'_c) = 3\mu'(\omega' l')^2 S^2(1-\eta) \tag{18}$$

Although the shear stress can be large at the surface of the vane, the rotating vane is not suitable for communition because only a small fraction of the flows is subjected to the high shear. On the other hand, shear degrading of suspensions can be a significant problem at high rotational speeds.

CONCLUSIONS

The integral momentum approach using the von Karman-Pohlhausen approximation for the boundary-layer flow on a vane appears to give fluid exit velocities in agreement with experimental data. These velocities were evaluated indirectly from photographs of the exiting jet.

Computational data show that the cubic term in the boundary-layer profile adds only a slight correction to a parabolic velocity profile. Assumption of a parabolic velocity profile leads to a simple analytical solution for the surface (or average) velocity [Equation (16*a*)] and the shear stress distribution [Equation (18)]. Since drop breakup and spray distribution are enhanced by higher exit velocities, these calculations show that higher angular velocities are advantageous, a fact known by spray disc manufacturers. However, the processing of shear degradable materials or suspensions can be adversely affected by the increased shear.

It is also evident that the use of a vane atomizer for production of an emulsion or dispersion is inefficient because only a small percentage of the fluid is subject to sufficient shear stress to cause dispersion.

NOTATION

A = ratio of average radial velocity to surface velocity
B = $1 + V_1^2$
G = velocity profile parameter $NQ^2r/(A^2S^3)$
h' = distance normal to vane, ft.
h = h'/l'
h'_v = depth of liquid on vane, ft.
h_v = h'_v/l'
l' = outside radius of vane, ft.
N = vane Reynolds number $(\omega' l'^2/\nu')$
N_{Re} = jet Reynolds number $(2R'_0\overline{V}'/\nu')$
Q' = volumetric flow per unit width on vane, sq.ft./sec.

Q = $Q'/\omega' l'^2$
R'_0 = jet radius, ft.
r' = radius, ft.
r = r'/l'
S' = surface velocity, V'_{rS}, ft./sec.
S = $S'/\omega' l'$
t' = time, sec.
t = $\omega' t'$, dimensionless time or rotational angle
V'_h = velocity normal to surface, ft./sec.
V'_r = radial velocity, ft./sec.
V_r = $V'_r/\omega' l'$
$\bar{V}'_0$ = average velocity at vane origin, ft./sec.
Z' = axial distance in jet

Greek Letters

ρ' = liquid density, lb.$_m$/cu. ft.
τ' = shear stress, lb.$_f$/sq. ft.
ν' = kinematic viscosity, sq. ft./sec.
μ' = viscosity, lb.$_m$/(ft.)(sec.)
ω' = angular velocity, rad./sec.

Subscripts

r, h = coordinate directions
0 = vane origin
1 = vane exit
S = surface

LITERATURE CITED

1. Duda, J. L., and J. S. Vrentas, *Chem. Eng. Sci.*, **22**, 855 (1967).
2. Goren, S. L., and S. Wronski, *J. Fluid Mech.*, **25**, 185 (1966).
3. Hallern, R. M., J. P. Johnston, and W. C. Reynolds, *ASME Paper No. 65-WA/FE-15* (1965).
4. Marshall, W. R., Jr., *CEP Monogr. Ser. No. 2*, **50** (1954).
5. Turner, H. E., and H. E. McCarthy, *AIChE J.*, **12**, 784 (1966).

Manuscript received June 9, 1969; revision received November, 1970; paper accepted November 19, 1970.

The Motion of Vapor Bubbles Growing in Uniformly Superheated Liquids

YUDA PINTO and E. JAMES DAVIS

Department of Chemical Engineering

Clarkson College of Technology, Potsdam, New York 13676

The motion of simultaneously rising and growing vapor bubbles in a uniformly superheated liquid is analyzed, and the predicted bubble velocities are shown to be in good agreement with available data. Using a quasisteady state approximation to describe the drag, and existing bubble growth theory to describe the growth rate, the equation of motion is solved for two ranges of bubble size encountered in nucleate boiling. For smaller bubbles ($R<0.04$ cm.) an analytical solution is obtained, and for larger bubbles ($R>0.07$ cm.) a numerical solution and analytical asymptotic solutions are obtained.

The motion of constant size bubbles in liquids has been widely studied, and the drag exerted on a bubble by the continuous phase has been examined both theoretically and experimentally for a wide range of bubble sizes. Considerably less information is available on the motion of growing or collapsing bubbles, although such motion is of interest in nucleate boiling, cavitation, gas bubble dissolution and chemical reaction in a liquid phase, effervescence, and other two-phase phenomena.

To predict heat and mass transfer rates associated with simultaneously growing and moving bubbles, it is necessary to have information on the translational velocity of the bubbles. It is the purpose of this paper to show that the unsteady state motion of growing bubbles can be predicted using information on the steady state motion of bubbles of constant size.

BUBBLE RISE VELOCITIES

Haberman and Morton (*1*) presented and discussed data on the terminal velocities of bubbles for a number of liquids, and their results were analyzed by Mendelson (*2*). The general behavior and ranges of interest are shown in Figure 1. The curve has been described quantitatively by Mendelson by considering the four regions indicated in the figure.

Region 1 ($R \lesssim 0.01$ cm.). Very small bubbles rise and behave like solid spheres, following Stokes' law ($N_{Re} < 1$),